High-energy electromagnetic follow-up of gravitational wave transient events

Barbara Patricelli[1,2], **Massimiliano Razzano**[1,2]
in collaboration with:
Giancarlo Cella[2], Elena Pian[3], Antonio Stamerra[3,4]

[1]University of Pisa
[2]INFN - Sezione di Pisa
[3] Scuola Normale Superiore di Pisa
[4]INAF-Osservatorio Astronomico di Torino

Congresso SIF 2015
21-25 Settembre, 2015
Roma

Mergers of compact objects

Mergers of compact objects (NSs and/or BHs) are the most promising sources for the first GW detection by Advanced LIGO and Advanced Virgo

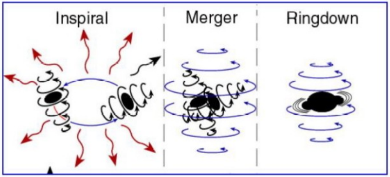

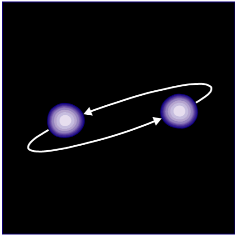

NS-NS and NS-BH mergers are expected to be associated with **short GRBs**

$\Rightarrow$

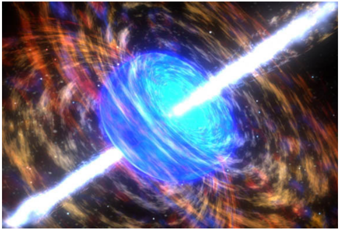

EM follow-up of GW events is a key tool to better understand the physics of compact objects and to unveil the nature of short GRB progenitors.

The Fermi Large Area Telescope

Credit: http://fermi.gsfc.nasa.gov/

- Energy range: 0.02-300 GeV
- Large field of view ($\sim$ 2.4 sr)

  $\Rightarrow$ this allows to cover the large error boxes in the sky position of GW candidates
- Accurate localization ($r_{68} \sim 0.8^{\circ}$ at 10 GeV on-axis)

  $\Rightarrow$ refinement of the localization of the GW event and alerts to other observatories

Step 1: simulation of the NS-NS mergers

NS-NS mergers

- NS-NS merger rates are dominated by the contribution from Milky Way-like galaxies (see e.g. O'Shaughnessy et al. 2010)
- $\rho_{galaxies}$=0.0116 Mpc^{-3} (Kopparapu et al. 2008)
- Simulated galaxies are uniformly distributed in volume
- Merging systems: `www.syntheticuniverse.org` (Dominik et al. 2012)
  NS-NS, Z=Z$_\odot$ and Z=0.1$\cdot$Z$_\odot$
  Standard model
- Merger rates: 23.5 Myr^{-1} (Z=Z$_\odot$) and 8.1 Myr^{-1} (Z=0.1$\cdot$Z$_\odot$) (Dominik et al. 2012)
- 1000 realizations, each one for a 1 year observing period

Step 2: GW detections and sky localizations

GW signals

- Each NS-NS merging system has the same sky position of the host galaxy
- We assume non-spinning systems
- TaylorT4 waveforms (Buonanno et al. 2009)

GW detections

- Detector configurations (aLIGO and AdV): 2016-2017 and 2019+ (design) (Aasi et al. 2013)
- Matched filtering technique (Wainstein 1962)
- trigger: at least 2 detectors
- Combined detector SNR threshold: 12
- GW localization with BAYESTAR (Singer et al. 2014)
- Independent duty cycle of each interferometer: 100 % and 80 %

Step 3: GRB simulations

GRB 090510 as a prototype:
it is the only short GRB to show an **extended emission (up to 200 s) at high energies (up to 4 GeV)**, as detected by *Fermi*-LAT (Ackermann et al. 2010, De Pasquale et al. 2010)

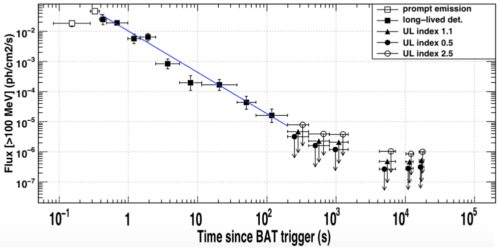

- light curve well fitted by a power law with a decay index α_t=1.38
- spectrum fitted by a power law with photon index α=-2.1

Step 3: GRB simulations

Assumptions

- All the merging NS-NS systems are progenitors of short GRBs.
- The total EM energy emitted in γ rays is: 10^{49} erg $\leq E_\gamma \leq 10^{53}$ erg.
- The extended emission of these GRBs has the same power law decay in time and the same spectral shape observed for GRB 090510.
- GRB 090510 is an on-axis GRB (θ=0).
- The simulated GRBs have random values of $\theta \Rightarrow$ we consider a simplified model of a point source moving along the jet axis at angle θ relative to the observer (Granot et al. 2002), with a constant Lorentz factor Γ=100[a] .

[a]this is a realistic for the early afterglow emission

- We re-scaled the HE flux of GRB 090510 above 100 MeV to take into account the different distances, total energies, and inclination angles of the progenitors.
- We estimated the integration time t_f needed for the simulated GRBs to have a fluence equal to the Fermi-LAT sensitivity.

Preliminary results: GW detections - I

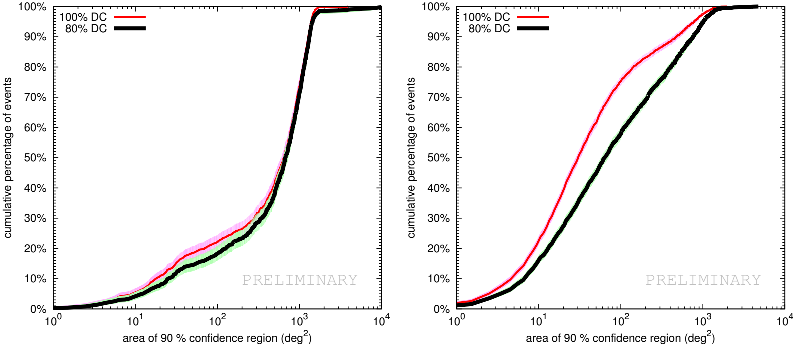

Figure: Cumulative histograms of sky localization areas for NS-NS systems at solar metallicity for the 2016-2017 (left) and the design (right) configuration of the interferometers.

Preliminary results: GW detections - II

2016-2017			
	Number of NS-NS detections	% of NS-NS Localized within 5 deg^2	% of NS-NS Localized within 20 deg^2
Aasi et al. 2013	0.006-20	2	5-12
Singer et al. 2014[a]	1.5	2	8
Sim., Z=Zsun, 80 % duty cycle	0.53 (0.006–1.7)[†]	$2.3^{+1.2}_{-0.8}$	$7.9^{+1.9}_{-1.5}$

Table: Expected GW detection rate and source localization for the 2016-2017 configuration, with an independent **80% duty cycle** of each interferometer.

[a] These estimates refer to the 2016 scenario.

[†] The range of GW detection rates reported in parenthesis has been estimated considering the highest range of NS-NS merger rates reported by Dominik et al. 2012, corresponding to model V12, sub-models A and B (Dominik et al. 2012).

Preliminary results: GW detections - III

2019+ (design)			
	Number of NS-NS detections	% of NS-NS Localized within 5 deg^2	% of NS-NS Localized within 20 deg^2
Aasi et al. 2013	0.2-200	3-8	8-28
Sim., Z=Zsun, 80 % duty cycle	7.5 (0.05–12.4)†	$7.6^{+0.7}_{-0.6}$	$27.6^{+1.1}_{-1.1}$

Table: Expected GW detection rate and source localization for the design configuration, with an independent **80% duty cycle** of each interferometer.

† The range of GW detection rates reported in parenthesis has been estimated considering the highest range of NS-NS merger rates reported by Dominik et al. 2012, corresponding to model V12, sub-models A and B (Dominik et al. 2012).

Preliminary results: Percentage of joint HE EM and GW detections

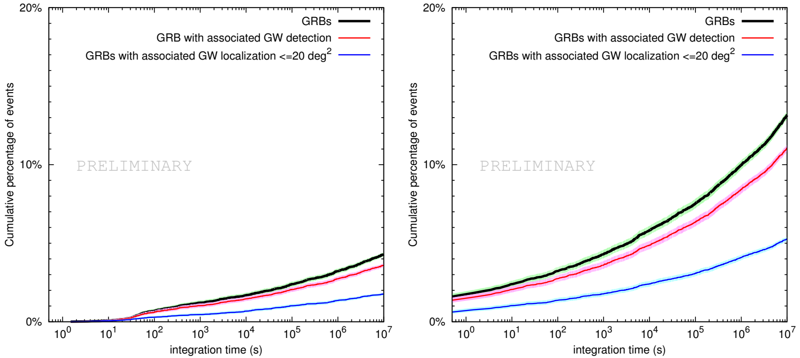

Figure: Left: cumulative histogram of the integration time needed for the simulated GRBs (in red), for the simulated GRBs with associated GW detection (in black) and with a sky localization ≤ 20 deg^2 (in blue) to be detected by the LAT. We assume $E_\gamma = 10^{49}$ erg and, for the GW detections, we consider the design scenario and a 100 % duty cycle of each interferometer. NS-NS systems at solar metallicity (standard model) are considered. Right: same as left, but we assume $E_\gamma = 10^{53}$ erg.

Conclusions

Conclusions

- We have estimated the GW detection rates and sky localizations for NS-NS mergers, finding values consistent with the ones reported in literature
- We have presented estimates of the joint HE EM and GW detection rates with *Fermi*-LAT

Next steps

- Investigation of the optimal HE EM follow-up strategies
- Extension of the work considering the other models by Dominik et al. 2012
- Extension to NS-BH merging systems
- Extension to other observatories (for example, ACT, *Swift* etc)

Backup slides

Backup slides

Short GRBs

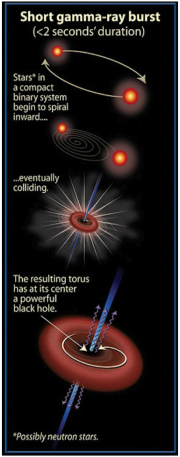
Short gamma-ray burst
(<2 seconds' duration)
Stars* in a compact binary system begin to spiral inward....
...eventually colliding.
The resulting torus has at its center a powerful black hole.
*Possibly neutron stars.

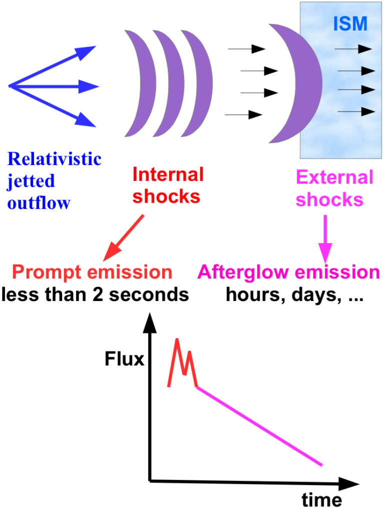
ISM
Relativistic jetted outflow
Internal shocks
External shocks
Prompt emission
less than 2 seconds
Afterglow emission
hours, days, ...
Flux
time

EM follow-up

EM follow-up of mergers is a key tool to better understand the physics of compact objects and to unveil the nature of short GRB progenitors.

GW alert → **Sky localization** → **EM follow-up**

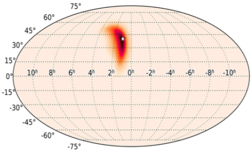

- Latency to generate GW alerts with sky localization: $\sim$ minutes
  $\Rightarrow$ EM observations mainly of the afterglow emission
- Localization uncertainties within tens to hundreds of square degrees
  $\Rightarrow$ **Wide field of view EM detectors are needed!**

The Advanced Virgo and Advanced LIGO sensitivities

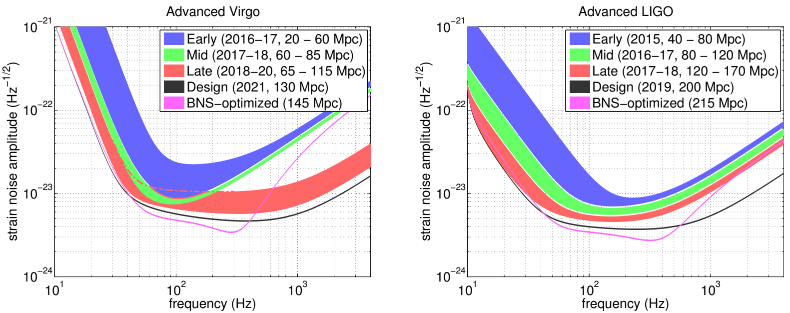

Aasi et al. (2013)

Fermi-LAT sensitivity to GRBs

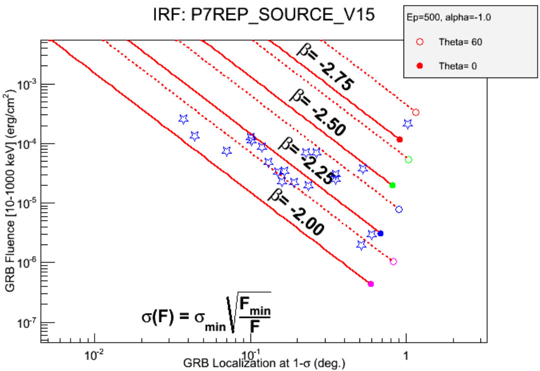

http://www.slac.stanford.edu/exp/glast/groups/canda/archive/p7rep_v15/lat_Performance.htm

- We extrapolated this sensitivity to the energy range 0.1-300 GeV
- We estimated the integration time t_f needed for the simulated GRBs to have a fluence equal to the Fermi-LAT sensitivity; we choose the value of sensitivity corresponding to a GRB localization of 1 deg, for Theta=0.

The Band function

$$N_E(E) = \begin{cases} A\left(\frac{E}{100keV}\right)^{\alpha} \exp\left(-\frac{E}{E_0}\right) & (\alpha-\beta)E_0 \geq E \\ A\left[\frac{(\alpha-\beta)E_0}{100keV}\right]^{(\alpha-\beta)} \exp(\beta-\alpha)\left(\frac{E}{100keV}\right)^{\beta} & (\alpha-\beta)E_0 \leq E \end{cases}$$

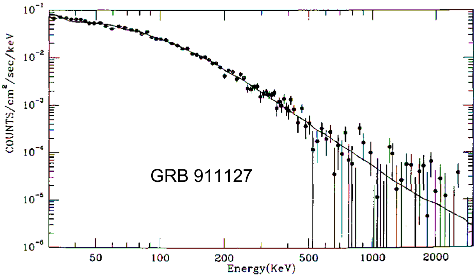

Band et al. (1993)

GW detections

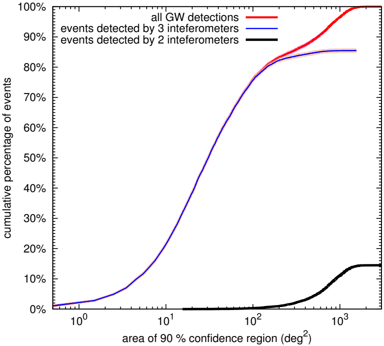

Figure: Cumulative histograms of sky localization areas for NS-NS systems at solar metallicity for the design configuration of the interferometers and with a 100% duty cycle.

Preliminary results: Percentage of joint HE EM and GW detections

Integration Time (s)	% of GRBs with HE EM detection	% of GRBs with HE EM and GW detections	% of GRBs with HE EM and GW detections, GW loc $\leq$ 20 deg^2
10	2.4 (0.1)	2.1 (0.1)	1.0 (0.1)
200	3.5 (0.9)	3.0 (0.8)	1.5 (0.3)
1000	4.3 (1.2)	3.6 (1.0)	1.8 (0.5)

Table: Expected percentages of EM and GW detections for the 2019+ (design) configuration, considering a 100 % duty cycle of the interferometers and assuming E_γ=10^{53} erg (10^{49} erg). NS-NS systems at solar metallicity (standard model) are considered.

GRB light curves

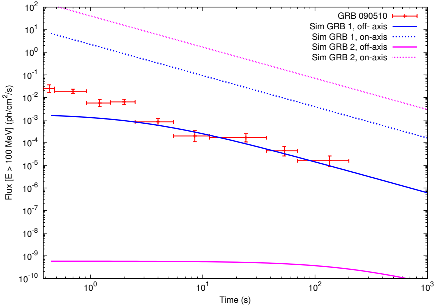

Figure: Flux time evolution of GRB 090510 (in red) and of two randomly extracted simulated GRBs (in blue and magenta) off axis (solid lines) and on axis (dashed lines); we assumed $E^{\gamma}_{EM} = 10^{53}$ erg.

	GRB1	GRB2
θ (deg)	2.4	13.9
z	0.035	0.013
GW loc (deg^2)	29.8	1.0
t_{f} (s)	2	4×10^6

Table: Inclination angle θ, redshift z, GW localization and integration time t_{f} of the two simulated GRBs shown in the Figure.